Influence of grain characteristics on the friction of granular shear zones

Karen Mair,[1] Kevin M. Frye, and Chris Marone[2]

Department of Earth Atmospheric and Planetary Sciences, Massachusetts Institute of Technology, Cambridge, Massachusetts, USA

Received 12 March 2001; revised 13 December 2001; accepted 18 December 2001; published 10 October 2002.

[1] Numerical models of granular shear show lower friction and a greater tendency for stick slip than laboratory studies designed to investigate fault mechanics. Here we report on laboratory experiments designed to reproduce the conditions of numerical models and to test the role that grain characteristics play in controlling frictional behavior. Friction and microstructural data are compared for direct shear experiments on thin layers (2–3 mm) of angular quartz sand and spherical glass beads. We study the effect of grain shape, roughness, size distribution, and comminution. In a nonfracture loading regime, sliding friction for smooth spherical particles ($\mu \sim 0.45$) is measurably lower than for angular particles ($\mu \sim 0.6$). A narrow particle size distribution (PSD) of spherical beads (105–149 μm) exhibits unstable stick-slip behavior, whereas a wide PSD of spheres (1–800 μm) and the angular gouge display stable sliding. At higher stress, where grain fracture is promoted, initially spherical particles become stable with accumulated slip, and friction increases to the level observed for angular gouge. We find that frictional strength and stability of a granular shear zone are sensitive to grain shape, PSD, and their evolution. We suggest that a low friction translation mechanism, such as grain rolling, operates in gouge composed of smooth particles. Our results show that the first-order disparities between laboratory and numerical studies of granular shear can be explained by differences in grain characteristics and loading conditions. Since natural faults predominantly contain angular gouge, we find no evidence for a fault-weakening mechanism associated with the presence of gouge. *INDEX TERMS:* 7209 Seismology: Earthquake dynamics and mechanics; 7215 Seismology: Earthquake parameters; 5112 Physical Properties of Rocks: Microstructure; *KEYWORDS:* friction, fault gouge, granular materials, stick slip, particle dynamics, strength

Citation: Mair, K., K. M. Frye, and C. Marone, Influence of grain characteristics on the friction of granular shear zones, *J. Geophys. Res.*, *107*(B10), 2219, doi:10.1029/2001JB000516, 2002.

1. Introduction

[2] Earthquakes occur on active faults in the brittle crust that are often perceived as discrete discontinuities (or seams) between intact country rock. However, natural faults commonly contain significant accumulations of granular wear material (gouge), making them mechanically and physically distinct from the surrounding rock. The nature and evolution of this granular wear material significantly affect mechanical strength, frictional stability, and the potential for seismic slip. To understand the mechanics of earthquakes and faulting, it is therefore essential to understand the behavior of gouge-filled fault zones.

[3] In this paper we investigate the dynamics of gouge-filled fault zones by studying shear in thin granular layers constrained within rigid boundaries. Many similar laboratory studies have been carried out, and much is known about the general frictional properties of gouge under geophysically relevant conditions (see *Marone* [1998] and *Scholz* [1998] for recent summaries). However, much of this work has focused on the effects of net shear displacement and shear localization, and relatively little is known about how specific grain characteristics influence the bulk frictional strength. A key problem is that the experimental configurations, designed to achieve high stresses, do not allow direct observation of the strain rate field during deformation. Thus the connection between frictional behavior and particle dynamics including rotation, translation, and fracture has to be inferred indirectly or from postexperiment microstructural observations.

[4] Numerical simulations offer the possibility of improving our understanding of the dynamics and kinematics of granular shear [*Pisarenko and Mora*, 1994; *Mora and Place*, 1994, 1998, 1999; *Scott*, 1996; *Morgan*, 1999; *Morgan and Boettcher*, 1999; *Aharonov and Sparks*, 1999]. These studies show that complex dynamics can arise from simple particle-particle interactions when large numbers of grains are considered. However, many of the existing numerical studies yield significantly different results from

[1]Now at Department of Earth Sciences, University of Liverpool, Liverpool, UK.

[2]Now at Department of Geosciences, Pennsylvania State University, University Park, Pennsylvania, USA.

0148-0227/02/2001JB000516$09.00

corresponding laboratory studies. In particular, numerical studies show lower frictional strength and a greater tendency for instability than laboratory studies. In one class of numerical simulations the observation of low friction has been linked to rolling in particles of simulated fault gouge [*Mora and Place*, 1999]. It has been suggested that these results may explain the apparent weakness of major faults, such as the San Andreas in California.

[5] There are several key differences between the numerical and laboratory studies. In particular, numerical shear zones are typically composed of idealized circular (two-dimensional, 2-D) particles that do not evolve, or evolve very little, during shear, whereas laboratory experiments are carried out on highly angular (3-D) particles undergoing pervasive fracture and comminution [*Sammis et al.*, 1987; *Marone and Scholz*, 1989]. We suggest that the apparent disparity between observations from laboratory and numerical studies of granular shear zones may be a consequence of these distinct differences in the nature of gouge and the deformation regimes imposed in both cases. For example, it is unclear whether idealized spherical particles typical in numerical models [*Mora and Place*, 1998, 1999; *Morgan and Boettcher*, 1999; *Morgan*, 1999; *Aharonov and Sparks*, 1999] and angular gouge used in laboratory experiments have a similar or distinct frictional response. Few laboratory studies have investigated the effect of grain shape on the behavior of sheared granular materials (but see *Mueth et al.* [2000]).

[6] The purpose of this paper is to investigate the influence of grain shape, roughness, and particle size distribution (PSD) on the frictional strength and stability of sheared granular layers. We carry out experiments at a range of normal stresses chosen to investigate both minimal and pervasive grain fracturing. Loading conditions are designed to reproduce both numerical modeling conditions and standard geophysical laboratory conditions. We observe systematic differences in the friction of angular and spherical granular materials. Our results are simple and indicate that much if not all of the first-order differences between numerical and laboratory experiments can be explained by differences in physical characteristics of gouge particles.

2. Experimental Method

[7] We shear granular layers between roughened steel blocks using a servohydraulic controlled direct shear apparatus (Figure 1). Extensive work has been done using this geometry [*Dieterich*, 1978, 1979; *Marone*, 1998], which we draw upon in this study. We use granular material to simulate wear products (gouge) commonly found in exhumed natural faults. The roughened boundary surfaces approximate the roughness of real faults and help promote shear throughout the layer rather than at the boundary. We apply and maintain constant normal force to the side blocks, then drive the center block at a specified load point velocity to initiate shear within the granular layer. Layers compact and dilate during shear reflecting the dynamic gouge reorganization required to accommodate shear. Layer thickness changes are continuously monitored together with shear and normal stresses. The coefficient of friction is defined as shear stress divided by normal stress. Additional experimental details are given by *Karner and Marone* [1998] and *Mair and Marone* [1999].

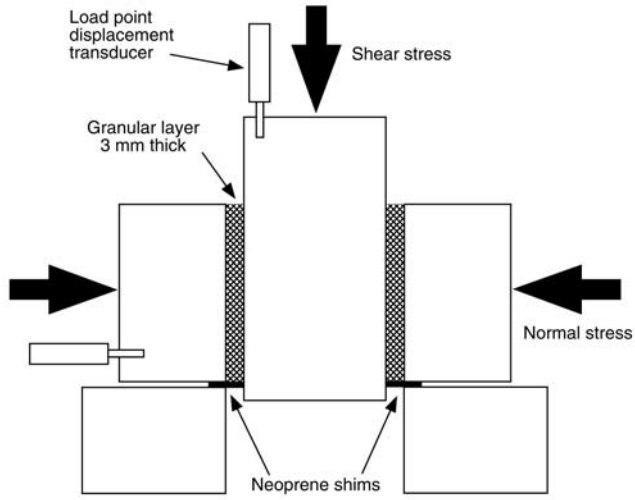

Figure 1. Schematic diagram of direct shear apparatus showing the 100 × 100 mm, 3-mm-thick granular layers sandwiched between rough steel bocks. The orientations of shear stress, normal stress, and load point displacement transducers are indicated.

[8] To investigate the influence of grain characteristics on sliding friction, we conducted identical direct shear experiments on 3-mm-thick layers of different simulated fault gouges. These gouges consisted of angular Ottawa sand (Figure 2a) and spherical soda-lime glass beads (Figure 2b). The Ottawa sand is a pure >99% quartz obtained from the U.S. Silica Company, Ottawa, Illinois, and has been used in previous laboratory studies of friction [*Karner and Marone*, 1998; *Richardson and Marone*, 1999; *Mair and Marone*, 1999]. We acquired precision glass spheres from Mo-Sci Corporation, Rolla, Missouri. Importantly, the particle size distribution (PSD) and mean grain size of the undeformed sand (Figure 2a) and spheres (narrow PSD, Figure 2b) are comparable, as are the compressive strengths of individual grains; hence the main difference between the gouges is the grain shape (Figure 2). A third gouge (Figure 2c) composed of spheres with a wide PSD was used to investigate the influence of grain size distribution (section 3.3) for constant spherical shape. This material had a lognormal PSD by weight in order to represent the PSD of a mature shear band [*An and Sammis*, 1994]. Experiments were carried out under a range of normal stresses ($\sigma_n = 5-50$ MPa) corresponding to regimes where previous work has indicated grain fracture to be minimal and pervasive, respectively [*Mair and Marone*, 2000]. Minimal grain fracture corresponds to the nonfracture regime generally invoked in numerical simulations, whereas a pervasive fracture regime is comparable to previous laboratory friction tests and potentially more applicable to natural conditions. Load point velocity ranged between 0.1 and 5000 μm/s. All experiments were carried out at room temperature and humidity. Other experimental conditions are presented in Table 1.

[9] Deformed gouge layers were impregnated with epoxy resin, and thin sections were prepared for microstructural analysis. Spherical beads required higher stresses to undergo pervasive fracture than angular quartz. This is perhaps due to a larger number of flaws in the quartz or to stress concen-

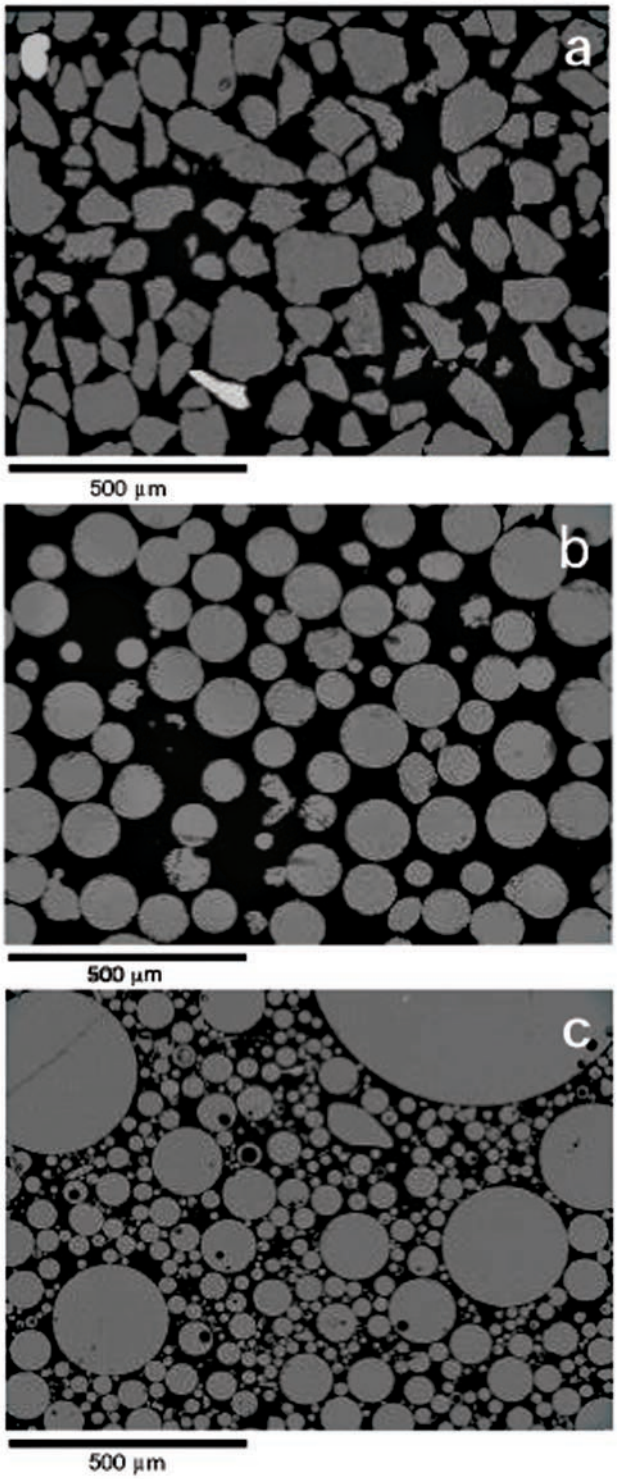

Figure 2. SEM photomicrographs of undeformed gouge: (a) angular grains and (b) spherical grains. The materials have a size range of 50–150 μm and 105–149 μm (grain diameter) respectively and means of ~110 μm and ~120 μm. (c) Spherical grains with a size range 1–800 μm (grain diameter) and a lognormal size distribution by weight with peak grain size at ~100 μm.

trations at grain irregularities. Grain fracture was recognized by significant audible cracking upon loading, and subsequent microstructural analysis. At a normal stress of $\sigma_n = 25$ MPa, few spherical grains fractured. Therefore the normal stress conditions used to achieve nonfracture and fracture of the two materials were as follows. For nonfracture regime, angular particles $\sigma_n < 10$ MPa; spherical particles $\sigma_n < 30$ MPa. For fracture regime, angular particles $\sigma_n > 10$ MPa; spherical particles $\sigma_n > 30$ MPa.

3. Results

3.1. Friction in Angular and Spherical Gouge

3.1.1. Low Stress (Nonfracture Regime)

[10] Initial shearing experiments were carried out at low normal stress ($\sigma_n = 5$ MPa) in the regime where grain fracture is minimal [*Mair and Marone*, 2000]. The friction coefficients for angular (Figure 2a) and spherical (Figure 2b) gouge material are plotted as a function of shear displacement in Figure 3. The main observation is that the coefficient of friction is markedly lower for the spherical gouge ($\mu \sim 0.45$) than the angular gouge ($\mu \sim 0.6$). In addition, the angular gouge exhibits stable sliding throughout, whereas the spherical gouge exhibits unstable stick slip. The angular gouge shown here was sheared at a constant load point velocity of $V = 5$ mm/s throughout. Previous work on the angular gouge showed that the base level of friction was comparable (~0.6) for 4 orders of magnitude range in load point velocity [*Mair and Marone*, 1999].

[11] We sheared spherical gouge at 10 μm/s initially and then changed velocity over several orders of magnitude to determine whether the instability observed was velocity-dependent. Figure 4 shows details of the periodic saw-tooth fluctuations in shear stress, typical of stick-slip cycles. The regular stick-slip events are characterized by a slow (elastic) increase in stress, a small inelastic rollover, and rapid

Table 1. Experiments[a]

Experiment	Grain Shape	Grain Diameter, μm	σ_n, MPa	V Range, μm/s	Sliding
		Nonfracture Regime			
m290	Ang	50–150	5	5000	stable
m302	Ang	50–150	5	5000	stable
m349	Sph	105–149	5	0.1–300	stick slip
m425	Sph	105–149	5	10–1000	stick slip
m428	Sph	105–149	5	10–1000	stick slip
m433	Sph	105–149	5	0.1–10	stick slip
m429	Sph	105–149	25	10–1000	stick slip
m431	Sph	105–149	25	10–1000	stick slip
m437	Sph	105–149	25	0.1–100	stick slip
m439	Sph	105–149	25	0.1–200	stick slip/stable
m351	Sph	105–149	25	10	stick slip
m446	Sph	1–800	5	10	stable
m444	Sph	1–800	5	1–20	stable (1 stress drop)
m445	Sph	1–800	5	10–20	stable (1 stress drop)
		Fracture Regime			
m268	Ang	50–150	25	1000	stable
m490	Ang	50–150	40	10	stable
m291	Ang	50–150	50	500	stable
m426	Sph	105–149	40	10–1000	stick slip/stable
m357	Sph	105–149	(40) 25	10	stick slip/stable

[a] Initial gouge layer thickness of 3 mm; Ang, angular; Sph, spherical; σ_n, normal stress; V, velocity.

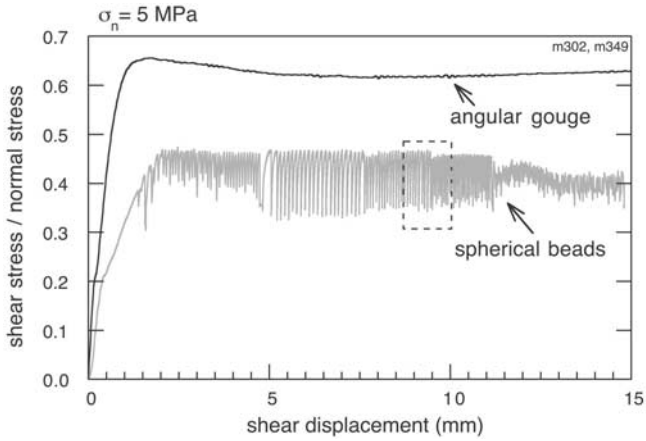

Figure 3. Friction as a function of shear displacement for angular and spherical grains at σ_n = 5 MPa. Grain fracture is minimal at this stress for both materials. Spherical grains show a lower value of friction coefficient and exhibit stick-slip behavior, whereas angular gouge slides stably with higher friction. Boxed region is enlarged in Figure 4.

dynamic stress drop that is accompanied by audible acoustic energy release. Figure 4 shows stick-slip cycles for two sliding velocities (V = 10 and 100 μm/s). Stress drop ($\tau_{max} - \tau_{min}$) decreases with increasing sliding velocity. Figure 5 shows stress drop measurements for many individual stick-slip events at a range of sliding velocities. The data are consistent with increased static yield strength due to the longer stick-slip recurrence interval at lower velocity. Our observations agree with previous work on gouge [*Wong and Zhao*, 1990] and mineral and rock surfaces [*Berman et al.*, 1996; *Karner and Marone*, 2000].

3.1.2. High Stress (Fracture Regime)

[12] Figure 6 shows friction versus shear displacement for angular and spherical gouge at higher normal stresses

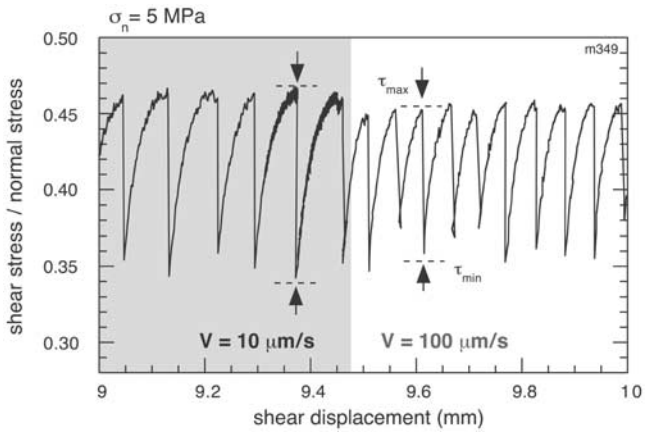

Figure 4. Enlargement of boxed region from Figure 3 illustrating details of stick-slip behavior for spherical gouge. Shaded and unshaded parts indicate slip rates of 10 and 100 μm/s, respectively. The stress drop ($\tau_{max} - \tau_{min}$) decreases with increased sliding velocity.

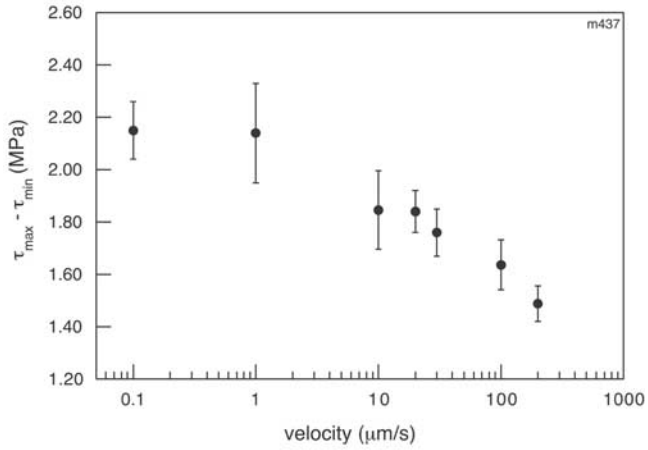

Figure 5. Stress drop ($\tau_{max} - \tau_{min}$) as a function of sliding velocity for spherical particles (σ_n = 25 MPa). Mean and ±1 standard deviation are plotted. Stress drop magnitude decreases with increasing sliding velocity.

(σ_n = 25 MPa and σ_n = 40 MPa, respectively) in the regime where grain fracture is important. As noted above, the stress required for the onset of pervasive fracture is slightly higher in spherical beads than angular gouge. Apart from comminution effects, we believe that the differences in nominal stress yield do not cause differences in frictional behavior. The angular gouge has a stable steady state friction level of 0.6, comparable to lower normal stress tests (Figure 3). Initially, the spherical material has low friction ($\mu \sim 0.45$) and shows stick-slip behavior, but with increasing shear, frictional strength increases and sliding stabilizes. After an engineering shear strain of ~8 (15-mm shear displacement),

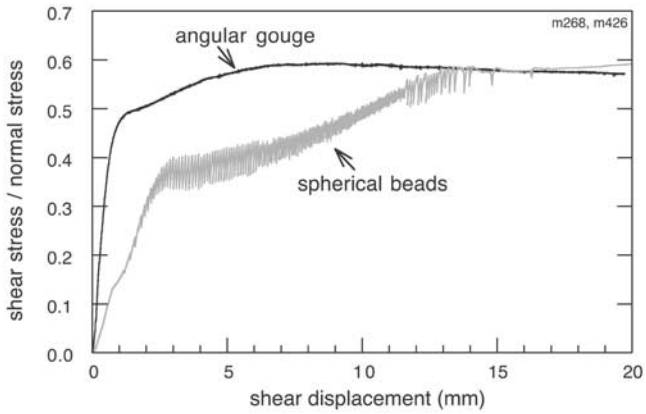

Figure 6. Friction versus shear displacement for angular and spherical gouge (initially 105–149 μm) deformed at σ_n = 25 MPa and σ_n = 40 MPa, respectively. Grain fracture is pervasive at these conditions in each material. With increasing slip the spherical granular material undergoes a transition from stick slip to stable sliding, and its frictional strength increases. Angular gouge exhibits stable shear throughout. Both tests are initially loaded at V = 10 μm/s; the spherical gouge includes subsequent changes in slip rate. A decrease in slip rate at 11-mm slip alters the stress drop amplitude and frequency of the instabilities.

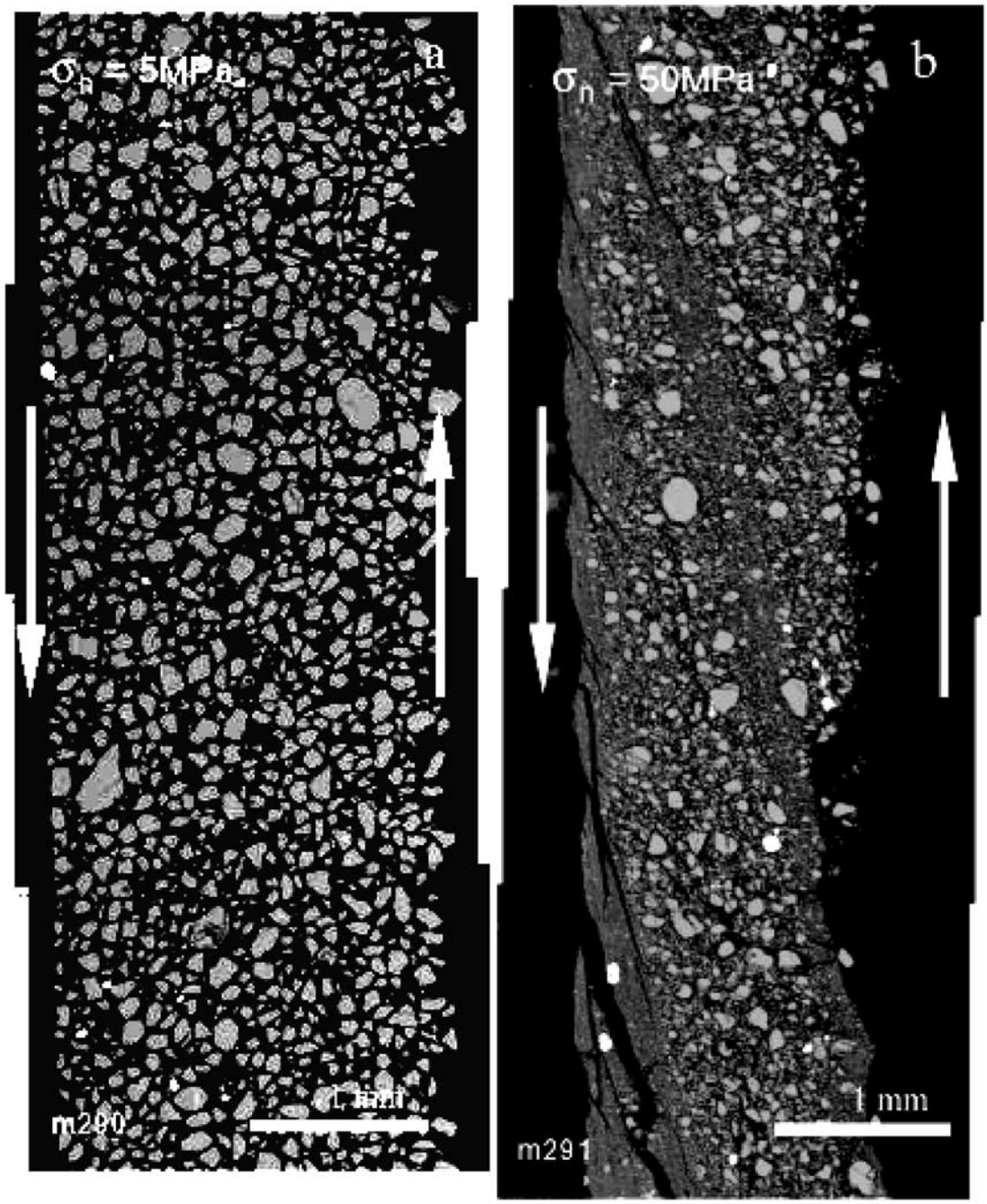

Figure 7. SEM photomicrograph of angular gouge deformed at (a) σ_n = 5 MPa and (b) σ_n = 50 MPa (redrawn after *Mair and Marone* [2000] with permission from Birkhaeuser Publishers Ltd.). In both cases, slip is 20 mm. Arrows indicate the sense of shear. Note the development of a distinct fabric in Figure 7b not seen in Figure 7a.

frictional strength is the same for angular and initially spherical particles.

3.2. Microstructural Development in Angular and Spherical Gouge

[13] Shear zone microstructures were investigated using scanning electron microscopy (SEM). Figure 7 shows photomicrographs of angular gouge deformed to 20-mm slip under normal stress of σ_n = 5 MPa (Figure 7a) and σ_n = 50 MPa (Figure 7b). The granular layers were initially identical (Figure 2a). Note the lack of grain fracture and the homogeneous texture at σ_n = 5 MPa (Figure 7a) compared with the distinct fabric developed at higher stress (Figure 7b). The structures in Figure 7b are typical of those observed in all tests conducted at σ_n > 25 MPa.

[14] SEM photomicrographs of initially narrow PSD spherical particles (Figure 2b) deformed at normal stresses of σ_n = 25 MPa and σ_n = 40 MPa are presented in Figures 8a and 8b, respectively. Similar to Figure 7, the low normal stress test indicates little grain fracture and no fabric

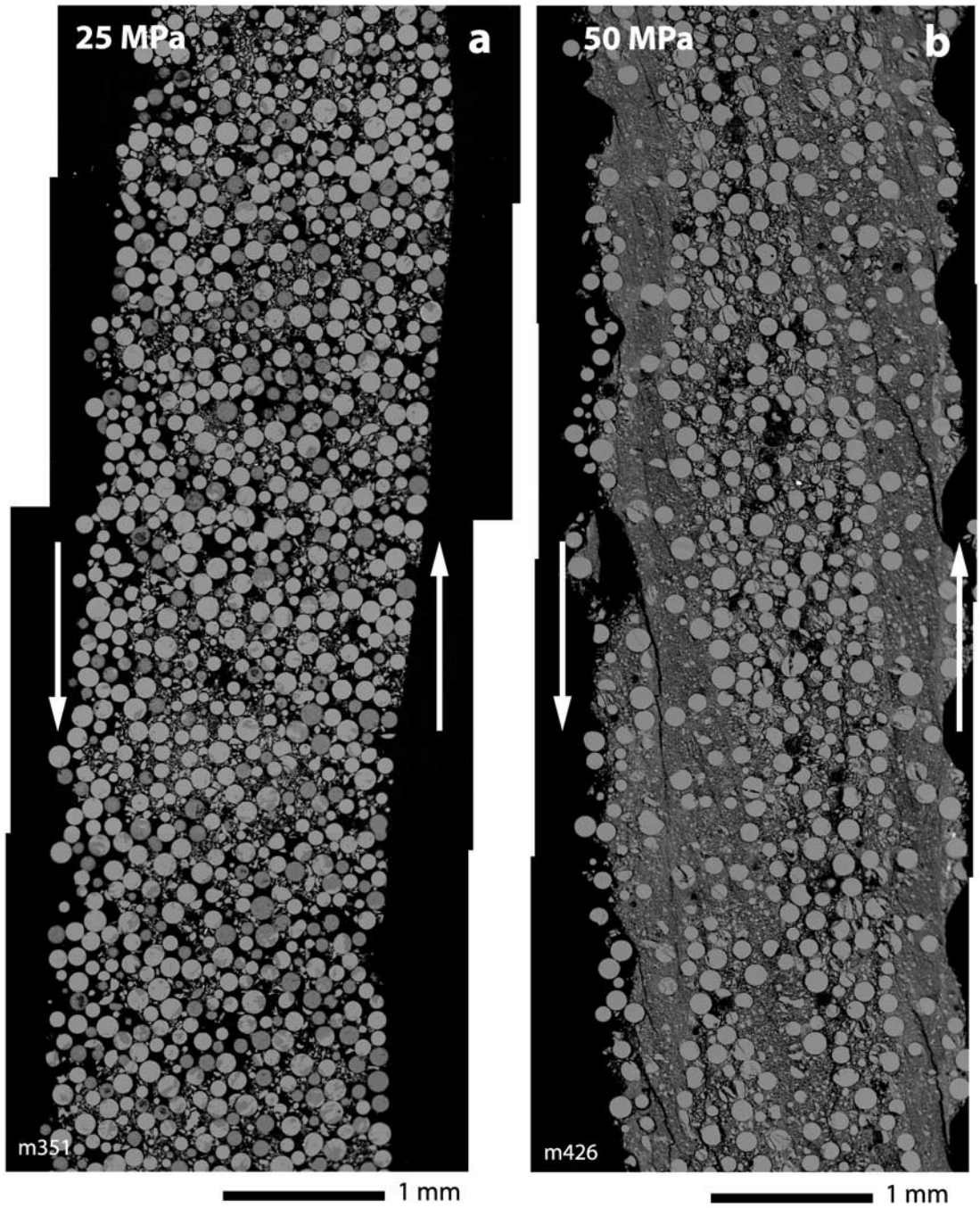

Figure 8. SEM photomicrograph of spherical gouge deformed at (a) σ_n = 25 MPa and (b) σ_n = 40 MPa. Slip is 20 mm in both cases, and the sense of shear is indicated by arrows. Note the development of a fabric in Figure 8b comparable to Figure 7b.

evolution, whereas the higher normal stress test exhibits a well-developed fabric. This fabric is highlighted by differences in grain size distributions, and although some relic spherical grains survive intact, many grains are no longer spherical.

[15] In both gouges at low normal stress (Figures 7a and 8a) grain size is representative of the undeformed material (Figures 2a and 2b, respectively). No clear microstructural signature of shearing is preserved, even after shear strains of ~12 (20-mm shear displacement). This indicates that few grains fracture and that nondestructive processes such as grain rolling and sliding accommodate the majority of deformation under these conditions. In contrast, significant fracture and grain size reduction clearly occurs at higher stress (Figures 7b and 8b). The resulting fabric is characterized by linear zones of intense comminution in boundary and Riedel orientation separated by relic zones of less deformed survivor grains. These features are characteristic of natural fault zones [*Logan et al.*, 1979; *Sammis et al.*, 1986; *An and Sammis*, 1994], and the comminution fabrics

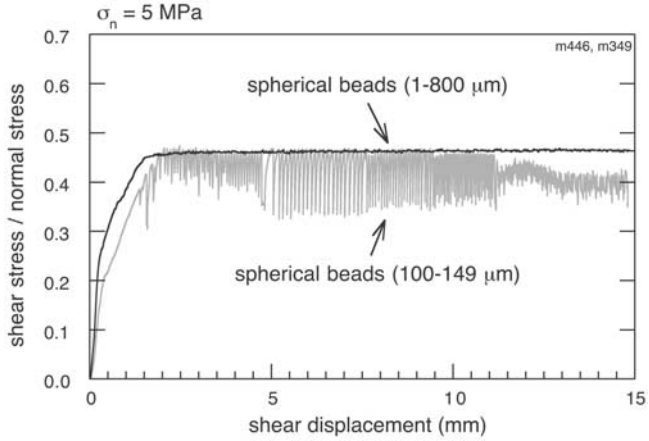

Figure 9. Friction versus shear displacement for two spherical gouges of narrow and wide size distributions deformed at σ_n = 5 MPa. A wide PSD promotes stable sliding at a level of $\mu \sim 0.45$, whereas gouge composed of a narrow PSD exhibits stick-slip sliding. Note that the peak frictional strength during stick slip (narrow PSD) is equal to the stable frictional strength of the wide PSD gouge.

are interpreted as zones of concentrated shear. Previous laboratory work on angular gouge [*Marone and Scholz*, 1989] and field observations [*Sammis et al.*, 1986, 1987; *An and Sammis*, 1994] indicate that a wide fractal PSD typically develops in these localized shear zones. In section 3.3 we isolate and consider the influence of PSD on friction for a constant grain shape.

3.3. Influence of Particle Size Distribution

[16] Our data show that spherical grains are markedly different than angular grains, exhibiting both lower friction and unstable stick-slip behavior (Figure 3). However, initially spherical material becomes stable and strengthens, approaching the behavior of an angular gouge as grain fracture and strain localization become significant. It is important to understand the processes responsible for this evolution. Candidate processes include (1) changes in grain-size distribution due to comminution; (2) particle roughening as spherical grains become more angular; and (3) the development of a strain localization fabric.

[17] We test these processes by changing the initial PSD for spherical particles. We use a lognormal PSD, which is intended to approach the PSD of a well-developed shear band [after *An and Sammis*, 1994] (Figure 2c). To isolate the influence of PSD, we deform this material at low stress where grains do not fracture; hence grain shape is constant throughout the test. If grain roughening due to comminution is the key factor, independent of PSD, we expect the wide PSD gouge will show the same frictional behavior as the narrow PSD gouge. If PSD is the important factor, then we expect to see strain hardening and stabilization in the wide PSD gouge.

[18] Our results (Figure 9) show that the coefficients of sliding friction for narrow and wide PSD spherical material are identical and measurably lower than that for angular gouge (Figure 3). Unlike the narrow PSD spherical particles, frictional sliding of wide PSD spheres is stable (Figure 9). This indicates that PSD is critical in achieving stable sliding but that angular grains are necessary to reach typical laboratory friction values of $\mu \sim 0.6$. We now discuss possible mechanisms for these observations.

4. Discussion

4.1. Frictional Strength

[19] The macroscopic frictional strength that we measure for angular quartz sand ($\mu \sim 0.6$) is comparable to that obtained in previous laboratory experiments. One of our most interesting observations, however, is that the friction level of a granular material composed of spherical grains is significantly lower than this ($\mu \sim 0.45$). The friction levels of spherical beads with both a narrow and broad particle size distribution are identical.

[20] This suggests that the kinematics of the angular and spherical particles are distinct. One explanation is that spherical grains accommodate strain preferentially by rolling, a highly efficient translation mechanism, leading to reduced macroscopic friction. Rolling is inhibited in angular grains, and thus translation must be accommodated by sliding and dilation. Our data indicate that spherical gouge is significantly weaker than angular gouge but that macroscopic friction is still >0.4.

[21] Interparticle friction (μ_p) of individual grains influences macroscopic sliding friction [*Morgan and Boettcher*, 1999]. It is tempting to account for the dramatic differences that we observe in friction by invoking differences in μ_p of the angular and spherical material; however, this alone is inadequate to explain our observations. We reason that the interparticle friction for spherical particles that survive intact (Figure 8a) and those that fracture at higher normal stress (Figure 8b) is essentially comparable and would lead to a similar macroscopic friction level if grain sliding alone were operating. However, Figure 6 indicates that the macroscopic friction level of spherical particles increases as grain comminution ensues, suggesting that an increase in angularity of the grains is a stronger effect. We suggest that as shape evolves due to comminution, the proportion of rolling to sliding decreases leading to higher friction. In addition, over the range studied, particle size distribution of spheres does not appear to influence frictional strength. Hence our observation of increased friction with progressive grain comminution is not due to evolution of PSD. Thus frictional strength appears to be a strong function of grain shape but not PSD during the shear of granular materials.

4.2. Frictional Stability

[22] For the stiffness of our shearing apparatus, angular gouge slides stably in all experiments, consistent with previous studies under similar conditions. We show that a narrow PSD of spherical material is unstable, exhibiting repetitive stick slip, whereas angular gouge and spherical material with a wider PSD are stable. In addition, stabilization of initially spherical (unstable) gouge occurs with grain comminution.

[23] We suggest that frictional stability is related to the nature of stress accommodation across a granular layer undergoing shear (Figure 10). We invoke the concept that stress chains or grain bridges preferentially support load in a sheared granular material [*Sammis et al.*, 1987; *Cates et al.*, 1998]. This model has recently proved useful in explaining

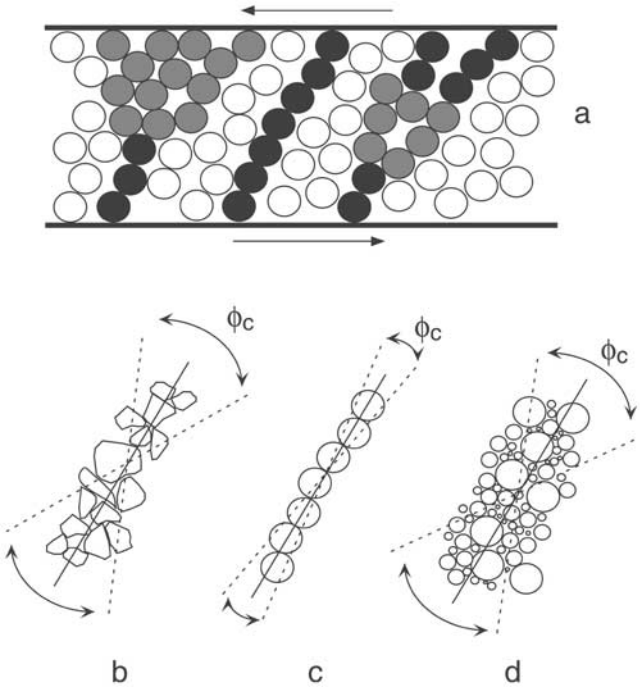

Figure 10. (a) Illustration of possible force chain geometries for a granular layer under shear. Dark gray indicates particles bearing high load; light gray indicates low to moderate load; and white indicates spectator particles not bearing appreciable load [see *Cates et al.*, 1998, Figure 1]. Note that stress can be supported by sets of localized chains of highly stressed particles (middle) or by diffuse webs of particles under lower stress (left, right). Examples of stress chains are shown for (b) angular gouge, (c) narrow PSD spherical particles, and (d) wide PSD spherical particles. Solid line indicates optimal chain orientation and dotted lines demark range of possible stable orientations; ϕ_c defines a critical angle for stress chains; outside this range, stress chains fail by interparticle slip or rolling. Note that Figures 10b and 10d have larger ϕ_c than Figure 10c. In addition, contact stresses are highest for Figure 10c.

observations from numerical modeling [*Morgan and Boettcher*, 1999] and laboratory experiments [*Karner and Marone*, 2001]. We propose that stress can alternatively be supported by diffuse webs of load-bearing particles, each particle carrying low to moderate stress, or sets of highly localized particle chains where fewer particles are involved but each experience much higher local contact stresses (Figure 10a). Importantly, both features are transient and persist only while they are favorably orientated (Figures 10b, 10c, and 10d).

[24] Our data can be explained by a model in which stress chains fail when they deviate beyond a critical angle (ϕ_c). Macroscopic boundary stresses are supported by systems of stress chains, which fail and reform repeatedly during shear. We posit that the critical angle (ϕ_c) is greater for diffuse stress chains than localized stress chains (Figure 10). A population of coexisting diffuse stress chains (Figures 10b and 10d) can have a range of orientations within ϕ_c. In contrast, for localized chains, critical angle (ϕ_c) is much smaller (Figure 10c) so a population of coexisting stress chains have very similar orientations. These chains are likely to collapse under approximately the same shear displacement, giving synchronous failure and a macroscopic stress drop.

[25] The nature of stress chains depends on grain characteristics and interactions such as co-ordination number Z (i.e. the number of other grains contacting each particle). Large Z implies diffuse stress chains (each particle carrying moderate load), whereas small Z corresponds to localized stress chains (composed of highly stressed particles). Numerical simulations [*Morgan and Boettcher*, 1999] indicate that coordination number increases and average contact force decreases with increasing fractal dimension (i.e., wider PSD) of gouge. We suggest that in our experiments, angular gouge and wide PSD spherical particles have large Z and develop diffuse stress chains (Figures 10b and 10d), whereas narrow PSD spherical particles have small Z and therefore develop highly concentrated stress chains (Figure 10c). When the narrow PSD gouge is sheared, these localized stress chains fail catastrophically due to geometric incompatibility, leading to dynamic stress drop and unstable stick-slip sliding.

[26] Our ideas are consistent with those of *Sammis et al.* [1987], who showed that similar sized neighboring particles (e.g., our narrow PSD gouge) have high probability of failure due to high individual contact stresses. In contrast, gouge with a range of particle sizes (e.g., our wide PSD gouge) can successfully distribute load over many particles, reducing stresses at individual contacts, in effect cushioning large particles and making failure less likely. In addition, instability is more likely for highly stressed particle chains since for a given local stiffness stick slip is favored by higher normal stress [*Dieterich*, 1978].

4.3. Comparison With Numerical Models

[27] Spherical particles show lower friction than identical experiments on angular gouge. Our results agree qualitatively with the numerical experiments of *Mora and Place* [1999] where grain shape is changed by bonding particles together. They also report that rougher particles exhibit higher macroscopic friction. The friction levels that we report for spherical material ($\mu \sim 0.45$) approach the levels often observed in numerical simulations where idealized circular particles are modeled [*Morgan*, 1999; *Aharonov and Sparks*, 1999; *Mora and Place*, 1998, 1999]. However, in the numerical models, friction is often 0.2–0.3, which is well below our observations. This may be a consequence of numerical work generally being done in two dimensions rather than three dimensions [*Morgan*, 1999].

[28] *Morgan and Boettcher* [1999, Figure 2] shows that an increase in fractal dimension D (i.e., wider PSD) promotes stable sliding, whereas low D (i.e., narrow PSD) has more numerous and larger stress drops. Our results are consistent, the stress drops that we observe being greater with narrower PSD and, in fact, absent for wider PSD gouge (Figure 9).

5. Conclusions

[29] Grain characteristics significantly affect the macroscopic friction of a granular material under shear. Gouge composed of smooth spherical particles has markedly lower

frictional strength than angular particles. Frictional stability is sensitive to the geometry of stress distribution throughout sheared layers and depends on particle size distribution and angularity. We show that the first-order discrepancies between laboratory and numerical studies may be explained by the differences in initial grain shape and loading regime. Our results indicate that gouges in natural faults may be significantly stronger than those predicted by numerical models using idealized smooth particles.

[30] **Acknowledgments.** The authors have enjoyed scientific discussions on this work with U. Mok, S. L. Karner, and J. Renner. We thank reviewers and editors for comments that led to an improved manuscript. This work was funded by National Science Foundation grants EAR-0001127 and EAR-0196570. K. Mair is supported by a Royal Society Dorothy Hodgkin Fellowship.

References

Aharonov, E., and D. Sparks, Rigidity phase transition in granular packings, *Phys. Rev. E*, *60*, 6890–6896, 1999.

An, L.-J., and C. G. Sammis, Particle size distribution of cataclastic fault materials from southern California: A 3-D study, *Pure Appl. Geophys.*, *143*, 203–227, 1994.

Berman, A. D., W. A. Ducker, and J. N. Israelachvili, Experimental and theoretical investigations of stick-slip friction mechanisms, in *Physics of Sliding Friction*, edited by B. N. J. Persson and E. Tosttati, pp. 51–67, Kluwer Acad., Norwell, Mass., 1996.

Cates, M. E., J. P. Wittmer, J.-P. Bouchaud, and P. Claudin, Jamming, force chains, and fragile matter, *Phys. Rev. Lett.*, *81*, 1841–1844, 1998.

Dieterich, J. H., Time-dependent friction and the mechanics of stick-slip, *Pure Appl. Geophys.*, *116*, 790–805, 1978.

Dieterich, J. H., Modeling of rock friction, 1, Experimental results and constitutive equations, *J. Geophys. Res.*, *84*, 2161–2168, 1979.

Karner, S. L., and C. Marone, The effect of shear load on frictional healing in simulated fault gouge, *Geophys. Res. Lett.*, *25*, 4561–4564, 1998.

Karner, S. L., and C. Marone, Effects of loading rate and normal stress on stress drop and stick-slip recurrence interval, in *Geocomplexity and the Physics of Earthquakes, Geophys. Monogr. Ser.*, vol. 120, edited by J. B. Rundle, D. L. Turcotte, and W. Klein, pp. 187–198, AGU, Washington, D.C., 2000.

Karner, S. L., and C. Marone, Frictional restrengthening in simulated fault gouge: Effect of shear load perturbations, *J. Geophys. Res.*, *106*, 19,319–19,337, 2001.

Logan, J. M., M. Friedman, N. Higgs, C. Dengo, and T. Shimamoto, Experimental studies of simulated gouge and their application to studies of natural fault zones, paper presented at Conference VIII: Analysis of Actual Fault Zones in Bedrock, Natl. Earthquake Hazards Reduction Program, Menlo Park, Calif., 1–5 April 1979.

Mair, K., and C. Marone, Friction of simulated fault gouge for a wide range of velocities and normal stresses, *J. Geophys. Res.*, *104*, 28,899–28,914, 1999.

Mair, K., and C. Marone, Shear heating in granular layers, *Pure Appl. Geophys.*, *157*, 1847–1866, 2000.

Marone, C., Laboratory-derived friction laws and their application to seismic faulting, *Annu. Rev. Earth Planet. Sci.*, *26*, 643–696, 1998.

Marone, C., and C. H. Scholz, Particle-size distribution and microstructures within simulated fault gouge, *J. Struct. Geol.*, *11*, 799–814, 1989.

Mora, P., and D. Place, Simulation of the frictional stick-slip instability, *Pure Appl. Geophys.*, *143*, 61–87, 1994.

Mora, P., and D. Place, Numerical simulation of earthquake faults with gouge: Toward a comprehensive explanation for the heat flow paradox, *J. Geophys. Res.*, *103*, 21,067–21,089, 1998.

Mora, P., and D. Place, The weakness of earthquake faults, *Geophys. Res. Lett.*, *26*, 123–126, 1999.

Morgan, J. K., and M. S. Boettcher, Numerical simulations of granular shear zones using the distinct element method, 1, Shear zone kinematics and the micromechanics of localization, *J. Geophys. Res.*, *104*, 2703–2719, 1999.

Morgan, J. K., Numerical simulations of granular shear zones using the distinct element method, 2, Effects of particle size distribution and interparticle friction on mechanical behavior, *J. Geophys. Res.*, *104*, 2721–2732, 1999.

Mueth, D. M., G. F. Debregeas, G. S. Karczmar, P. J. Eng, S. R. Nagel, and H. M. Jaeger, Signatures of granular microstructure in dense shear flows, *Nature*, *406*, 385–388, 2000.

Pisarenko, D., and P. Mora, Velocity weakening in a dynamical model of friction, *Pure Appl. Geophys.*, *142*, 447–466, 1994.

Richardson, E., and C. Marone, Effects of normal force vibrations on frictional healing, *J. Geophys. Res.*, *104*, 28,859–28,878, 1999.

Sammis, C. G., R. H. Osborne, J. L. Anderson, M. Banerdt, and P. White, Self-similar cataclasis in the formation of fault gouge, *Pure Appl. Geophys.*, *124*, 51–77, 1986.

Sammis, C. G., G. King, and R. Biegel, The kinematics of gouge deformation, *Pure Appl. Geophys.*, *125*, 777–812, 1987.

Scholz, C. H., Earthquakes and friction laws, *Nature*, *391*, 37–42, 1998.

Scott, D. R., Seismicity and stress rotation in a granular model of the brittle crust, *Nature*, *381*, 592–595, 1996.

Wong, T., and Y. Zhao, Effects of load point velocity on frictional instability behavior, *Tectonophysics*, *175*, 177–195, 1990.

K. M. Frye, Department of Earth Atmospheric and Planetary Sciences, Massachusetts Institute of Technology, Cambridge, MA 02139, USA.

K. Mair, Department of Earth Sciences, University of Liverpool, 4 Browlow Street, Liverpool L69 3GP, UK. (k.mair@liverpool.ac.uk)

C. Marone, Department of Geosciences, Pennsylvania State University, University Park, PA 16802, USA.